

## MgF<sub>2</sub>/CeO<sub>2</sub> 이중반사방지막을 이용한 BCSC태양전지의 효율향상과 최적화

### Optimization and Efficiency Improvement of BCSC Solar Cells Using MgF<sub>2</sub>/CeO<sub>2</sub> Double Layer Antireflection Coatings

이육재\*, 임동건\*, 이준신\*  
(W.J.Lee\*, D.G.Lim\*, J.Yi)

#### Abstract

This paper describes an efficiency improvement of buried contact solar cell (BCSC) with a structure of MgF<sub>2</sub>/CeO<sub>2</sub>/Ag/Cu/Ni grid/n<sup>+</sup> emitter/p-type Si base/P<sup>+</sup>/Al. Theoretical and experimental investigations were performed on a double layer antireflection (DLAR) coating of MgF<sub>2</sub>/CeO<sub>2</sub>. We investigated CeO<sub>2</sub> films as an AR layer because they have a proper refractive index of 2.46 and demonstrate the same lattice constant as Si substrate. An optimized DLAR coating showed a reflectance as low as 2.04 % in the wavelengths ranged from 0.4 μm to 1.1 μm. BCSC cell efficiency was improved from 16.2 % without any AR coating to 19.9 % by employing DLAR coatings. Further details on MgF<sub>2</sub>/CeO<sub>2</sub> DLAR coatings on the BCSC cells are presented in this paper.

**Key Words** : (Buried Contact Solar Cell)BCSC; (Double Layer Antireflection)DLAR, Passivation, Reflective Index.

#### 1. Introduction

Optical losses in solar cells come from three major sources such as a surface reflection, top grid shadowing, and inadequate absorption by either excess energy photons or weak energy photons [1]. We used buried contact solar cell (BCSC) structure to reduce top grid shadowing and weak energy photon losses. High efficiency solar cell can be obtained by employing a double layer antireflection (DLAR) coating for a reduction of the reflected percentage of incident light beams. Many research groups investigated on a double

layer AR (DLAR) coatings[2-5]. Among the various sets of DLAR coating, MgF<sub>2</sub>/ZnS, MgF<sub>2</sub>/TiO<sub>2</sub>, and SiO<sub>2</sub>/ Si<sub>3</sub>N<sub>4</sub> have been reported to be the best choice for a minimum reflectance. This paper studied a DLAR coating with a MgF<sub>2</sub>/CeO<sub>2</sub>/Cz-Si structure. We employed CeO<sub>2</sub> films because it shows a proper refractive index for the bottom AR layer and exhibits the same lattice constant as Si. There has been a successful epitaxial Si growth on CeO<sub>2</sub>/Si substrate. Since dangling bonds at Si surface can be passivated with CeO<sub>2</sub> films, we expect CeO<sub>2</sub> can be very effective in reducing surface state recombination of Si solar cells. Because excess energy photons are either absorbed or recombined at the surface of solar cells, we try to search for the AR

\* 성균관대학교 전기전자컴퓨터공학부  
(경기도 수원시 장안구 천천동 300번지)  
Fax: 031-290-7159  
E-mail : lujwon@hanmail.net)

materials and their processing conditions which can give the best interface property between AR layer and Si surface. A theoretical optimization process and experimental verification were carried out using a DLAR coating of MgF<sub>2</sub>/CeO<sub>2</sub>/Cz-Si BCSC. DLAR coated BCSC conversion efficiency was compared to a BCSC with a single AR layer of SiO<sub>2</sub> and to a BCSC without any AR layer.

## 2. Experiment

We used (100) Cz c-Si wafers with a size of 6", thickness 500 μm, resistivity about 0.5 Ω-cm. To minimize reflection losses, the top surface of wafers was chemically textured in 2% NaOH and 2-propanol solution. Emitter diffusion was carried out in a diffusion furnace by using phosphorus pentoxide solid source. The metal grid was defined by scribing deep grooves through the masking oxide. Nd:YAG power laser was employed to form grooves of 20~25 μm width and 40~80 μm depth. After chemical etching of the grooves to remove residues generated during laser grooving, a heavy phosphorus diffusion was carried out on a front metal contact regions. Aluminium was deposited onto rear side of the BCSC by electron beam evaporation and sintered to form an Ohmic contact and back surface field. The wafers were immersed in the buffered HF acid bath to remove all the oxide from the grooves (named as deglazing step). The buffered etch solution was composed of hydrofluoric acid (49% HF) and ammonium-fluoride (40% NH<sub>4</sub>F). To deposit a thin layer of nickel on the bare silicon surface in the grooves and on the rear surface we used ammonia based nickel source for electroless plating solution. The pH of the solution was maintained above 8.5 and the temperature was kept between 85°C and 90°C. After nickel plating wafers were sintered at 300~400°C in an inert atmosphere to form a good electrical and mechanical contact between the silicon and the nickel. Table 1 shows the BCSC cell fabrication procedures employed in this paper. CeO<sub>2</sub> thin films were RF sputter deposited using a Ce metallic target with a diameter of 2" and 99.9 % purity.

Table 1. Fabrication Procedure of Investigated BCSC and DLAR Coating.

Parameter	Eff.(%)	V <sub>oc</sub> (V)	J <sub>sc</sub> (mA/cm <sup>2</sup> )	FF (%)
No AR	16.2	0.57	19.8	71
SiO <sub>2</sub>	18.3	0.58	22.1	72
MgF <sub>2</sub> / CeO <sub>2</sub>	19.9	0.58	22.6	75

MgF<sub>2</sub> films were evaporated at a base pressure of low 10<sup>-6</sup> Torr. We investigated the surface morphology and refractive index of each layer using AFM, SEM, and ellipsometer. Prior to the actual DALR formation on the BCSC, we optimized the thickness of each layer in accordance with optical theory. Crystallographic properties were characterized using a XRD system of Mac Science M18XHF-SRA with an input power of 40 kV. The XRD scan angle was ranged from 20 to 70 degree with a speed of 8.0 deg/min. Electrical properties for CeO<sub>2</sub> and MgF<sub>2</sub> films were evaluated by C-V and I-V measurements. Refractive index was measured by an ellipsometer of Gaertner Scientific Cooperation L6B-85B with a wavelength of 632.8nm.

## 3. Results and Discussions

Crystal structures of the DLAR were investigated for various substrate temperatures. Fig. 2 shows the XRD results on CeO<sub>2</sub> and MgF<sub>2</sub> films grown at various substrate temperatures. CeO<sub>2</sub> film structure displayed a (111) preferential orientation. XRD results show that the CeO<sub>2</sub> crystalline peak appears as in crystalline Si peak positions. Having the same lattice constant and crystal structure, we expect to reduce the surface states between CeO<sub>2</sub> and Si substrate. MgF<sub>2</sub> films were grown as an amorphous state at RT. As substrate temperature increased above 100 °C, MgF<sub>2</sub> films also showed a (111) preferred orientation. XRD and ellipsometer measurements on CeO<sub>2</sub> films indicated that a film growth temperature is the most importance factor for the film property modulations.

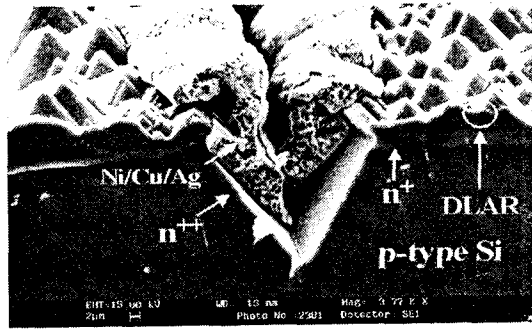


Fig. 1. SEM photograph showing the cross-sectional view of the fabricated BCSC. The buried contact metals were deposited using an electroless chemical plating of Ni,Cu and Ag.

Table 2 shows refractive indices for  $\text{CeO}_2$  and  $\text{MgF}_2$  films with a variation of growth temperature. The film growth temperature as demonstrated in Table 2 less influences on a refractive index of  $\text{MgF}_2$  than  $\text{CeO}_2$  film. We optimized the thickness of each layer and calculated reflectance of DLAR coating using classical optic theory.

Table 2. Refractive Indices of  $\text{CeO}_2$  and  $\text{MgF}_2$  Films.

Material	Variable	Refractive index
$\text{CeO}_2$	$T_s = \text{RT}$	2.352
	$T_s = 100^\circ\text{C}$	2.702
	$T_s = 300^\circ\text{C}$	2.780
	$T_s = 400^\circ\text{C}$	2.467
$\text{MgF}_2$	$T_s = \text{RT}$	1.386
	$T_s = 100^\circ\text{C}$	1.386
	$T_s = 200^\circ\text{C}$	1.385

For the investigated substrate temperatures, the crystalline structure of the  $\text{CeO}_2$  films displayed a (111) preferred orientation

The second and third best choice of  $\text{MgF}_2/\text{CeO}_2$  DLAR coating gave a reflectance equal to  $R_{\text{avg}}=2.18\%$  and  $R_{\text{avg}}=2.75\%$  for RT and  $100^\circ\text{C}$ , respectively.

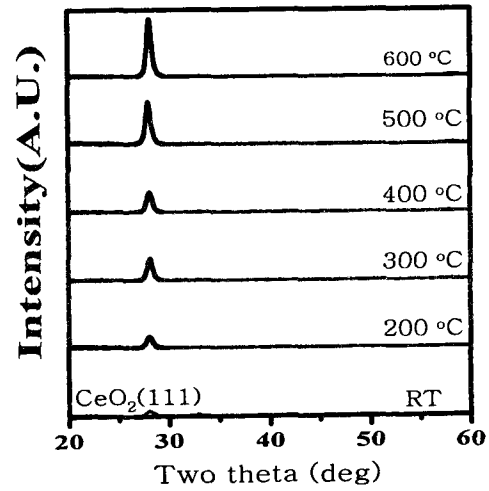


Fig. 2. XRD results for the  $\text{CeO}_2$  films on a Si substrate as a function of substrate temperature.

These results lead us to fix a substrate temperature of  $400^\circ\text{C}$  in the deposition of  $\text{CeO}_2$ . Metal-insulator-semiconductor type capacitors were investigated to probe  $\text{CeO}_2$  film qualities such as leakage current, breakdown field, oxide charge, and interface states (Dit). Leakage current of  $\text{CeO}_2$  film was stayed less than  $5 \times 10^{-6} \text{ A/cm}^2$  at an electric field of  $500 \text{ kV/cm}$ .  $\text{CeO}_2$  film grown at  $300^\circ\text{C}$  exhibited a breakdown field higher than  $3.5 \text{ MV/cm}$ .

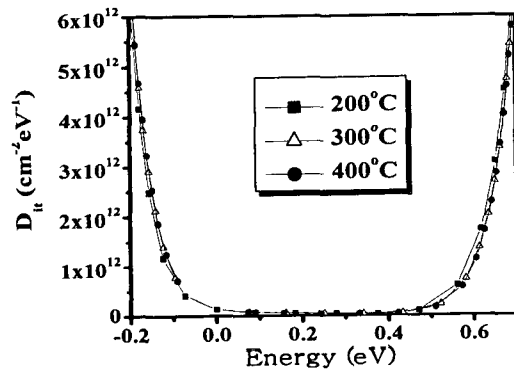


Fig. 3. Interface trap charge density vs. energy extracted from the C-V analysis for the  $\text{Al}/\text{CeO}_2/\text{p-type Si}$  MIS capacitors. The  $D_{it} \text{ eV}^{-1}$  for the different  $\text{CeO}_2$  film growth temperatures.

Fig. 3 shows C-V characteristics of CeO<sub>2</sub> films grown at 400°C that illustrates the lowest Dit as 8.74x10<sup>10</sup> cm<sup>-2</sup>eV<sup>-1</sup>. For most of capacitors, we observed that Dit calculated by Terman method stays around 10<sup>11</sup> cm<sup>-2</sup>eV<sup>-1</sup>. Low Dit can be explained by the close lattice mismatch between CeO<sub>2</sub> and Si substrate. This result of CeO<sub>2</sub> capacitor promises an excellent surface passivation effect. Thereby, reduced surface recombination is expected for solar cells. With an input power of 50 mW/cm<sup>2</sup>, we measured L-I-V characteristics of BCSC with and without AR coating.

Fig. 4 displays L-I-V curves for three different surface conditions. Short circuit current density of BCSC was improved from 16.2 mA/cm<sup>2</sup> without AR layer to 19.9mA/cm<sup>2</sup> for a DLAR coated BCSC. DLAR contributed to improve a conversion efficiency of BCSC by 3.7 % with an increased current density and fill factor. Table 3 lists cell parameters for the different AR types.

Table. 3. Cell Parameters of the investigated BCSC.

No	Process steps
1	Saw damage removal
2	Texturing and chemical cleaning
3	Emitter diffusion
4	Oxidation
5	Front laser scribing
6	Groove etching and diffusion
7	Rear aluminum deposition
8	Al sintering/Deglazing
9	Nickel/Copper/Silver plating
10	Edge isolation
11	MgF <sub>2</sub> /CeO <sub>2</sub> DLAR coating
12	Cell characterization

#### 4. Conclusion

This paper demonstrated an optimum condition of MgF<sub>2</sub>/CeO<sub>2</sub> DLAR and effect of DLAR coatings on randomly textured Cz Si wafers aiming at a low cost and high conversion efficiency of solar cells. Advantages of using CeO<sub>2</sub> film were introduced as an alternative material for

conventional ones like SiO<sub>2</sub>, TiO<sub>2</sub>, and Si<sub>3</sub>N<sub>4</sub>. The CeO<sub>2</sub> deposited at 400°C exhibited the a strong (111) preferred orientation and the lowest surface roughness of 6.87 Å.

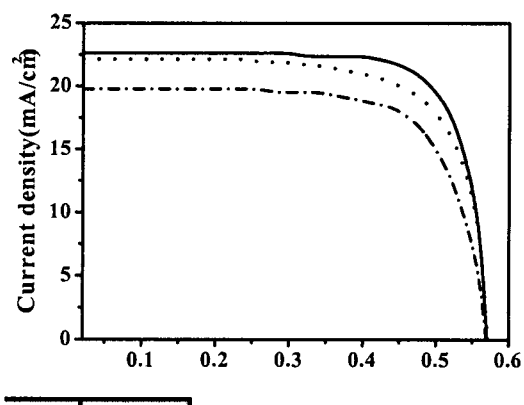


Fig. 4. The L-I-V characteristics of BCSCs for three different surface conditions: MgF<sub>2</sub>/CeO<sub>2</sub> DLAR, SiO<sub>2</sub> SLAR, and without an AR layer. The BCSC's efficiency improved from 16.2% to 19.9% when DLAR coatings were used.

Optimized refractive indices were given as 1.386 for MgF<sub>2</sub> and 2.467 for CeO<sub>2</sub>. We illustrated a MgF<sub>2</sub>/CeO<sub>2</sub> coating can reduce reflectance as low as 2.04 % in the wavelength regions of 0.4~1.1 μm and demonstrated the BCSC cell efficiency of 19.9 %. Side effect of using CeO<sub>2</sub>/Si AR coating was a low interface state of 10<sup>11</sup> eV<sup>-1</sup>cm<sup>2</sup>.

#### 참고 문헌

- [1] A. Goetzberger, J. Knobloch, B. Vob, R. Waddington, Crystalline Silicon Solar Cells, John Wiley and Sons, New York, p.89, (1998).
- [2] H. G. Shanghogue, S. N. Prasad, C. L. Nagendra, G. K. M. Thutupalli, Thin Solid Film 320, 290, (1998).
- [3] J. Zahao, Martin A. Green, IEEE Trans. Electron Devices 38, 1925, (1998).
- [4] Zhizhang Chen, Peyman Sana, Jalal Salami, Ajeet Rohagi, IEEE Trans. Electron Devices 40 1161.(1993).
- [5] G. Zhang, J. Zhao, M. A. Green, Solar Energy Materials and Solar Cells 51, 393, (1998).